



Hydrocarbon Reservoir Characterization of 'UDI' Field, Western Niger Delta

N. E. Osuya¹ and J. O. Ayorinde^{2*}

¹*Department of Petroleum Geoscience, Pan African University for Life and Earth Sciences Institutes,
University of Ibadan, Nigeria.*

²*Department of Geology and Mineral Sciences, University of Ilorin, Kwara State, Nigeria.*

Authors' contributions

This work was carried out in collaboration between both authors. Author NEO designed the study, performed the statistical analysis, wrote the protocol and wrote the first draft of the manuscript. Author JOA manages the analyses, prepared and edited the manuscript for submission. Both authors read and approved the final manuscript.

Article Information

DOI:10.9734/JGEESI/2020/v24i230198

Editor(s):

(1) Dr. Ioannis K. Oikonomopoulos, Hellenic Petroleum, Greece.

Reviewers:

(1) Nelson Enrique Barros Galvis, University of Atlantico, Colombia.

(2) Pablo Henrique dos Santos Picapedra, Universidade Estadual do Oeste do Paraná, Brazil.

(3) Breno Barra, Federal University of Santa Catarina, Brazil.

Complete Peer review History: <http://www.sdiarticle4.com/review-history/55238>

Received 29 December 2019

Accepted 05 March 2020

Published 18 March 2020

Original Research Article

ABSTRACT

The increasing demand for petroleum products has posed a challenge to the search for oil and gas. This search for hydrocarbon has developed due to advances in computational techniques to evaluate the probability of hydrocarbon proneness of a basin, thereby limiting the risk factor associated with hydrocarbon. This study was therefore designed to assess the hydrocarbon potential and generate a static reservoir model of UDI Field, Onshore Niger Delta. Well, the correlation was carried out to establish stratigraphic continuity of the reservoir sand bodies. The identified potential reservoir intervals were tied to the seismic data using available check shot survey data. With a good match achieved, seismic events were interpreted through paying attention to reflection continuity, amplitude and frequency. Interpreted horizons were converted to surfaces using a convergent interpolation algorithm. Faults within the Field showed a dominant East-West trend with two (2) major faults and five (5) minor ones. A Pixel-based facies model was built based on the normal distribution of the upscaled lithofacies log using the Sequential Indicator Simulation algorithm. Petrophysical models were built by constraining the petrophysical logs to the facies models using Sequential Gaussian simulation algorithm.

*Corresponding author: E-mail: ayorinde.jo@unilorin.edu.ng;

Four potential reservoir intervals, A100, A125, A150 and A200 were delineated. Average petrophysical parameters were computed for all the four intervals and the results revealed the reservoir intervals to be of good quality. Sand A100 has the highest average porosity value of 29.4%, while Sand A200 has the lowest value of 25.3%. Net-to-gross ratio also follows the pattern of decreasing value with depth. Sand A150 has the highest average gross thickness value, 170.4 m, while Sand A200 has the least thickness of 80.5 m. The net-to-gross ratio preserved the pattern of gross thickness and this resulted in Sand A150 still having the highest Net thickness and Sand A200 having the least Net sand thickness. The relatively large net sand thicknesses, high net-to-gross ratio values and the high porosity values all support the reservoir intervals within UDI Field to be of good quality.

Extrapolations of reservoir properties away from good control honored the geological interpretation of reservoir Sand A125 thereby reducing the subsurface reservoir uncertainties.

The availability of pressure data of the reservoir will help in establishing whether the reservoir is compartmentalized and hence the model can be updated to accommodate the effect of compartmentalization.

Keywords: Hydrocarbon reservoir; stratigraphic continuity; seismic data; petrophysical parameters.

1. INTRODUCTION

The search for more hydrocarbon exploration and production has been improved due to advances in computational techniques to evaluate the probability of hydrocarbon proneness of a basin, thereby limiting the risk factor associated with hydrocarbon.

The production of oil and gas in the Niger Delta is from the accumulation in the pore spaces of reservoir rock, usually sandstone and unconsolidated sand of Agbada formation Beka et al. [1]. This formation is characterized by alternating sandstone and shale with rock units varying in thickness from 100 ft to 15000 ft. The sand formation is mainly hydrocarbon reservoir with shale providing lateral and vertical seals. Without a doubt, there are continuous subsurface uncertainties and challenges of geological reservoir models and erroneous interpretations often associated with the already identified reservoirs in any sedimentary basin.

1.1 Geology of the Study Area

The Niger Delta is situated in the Gulf of Guinea on the west coast of Central Africa. The delta built out into the Atlantic Ocean at the mouth of the Niger-Benue River system during the Tertiary. Accumulation of marine sediments in the basin probably commenced in Albian time (199 Ma - 112 Ma), after the opening of the South Atlantic Ocean during the break-up of the African and American continents [2]. The Niger Delta is located in the southern part of Nigeria between latitudes 4°00'N and 6°00'N and longitudes 3°00'E and 9°00'E. It is bounded in the south by the Gulf of Guinea and in the North

by older (Cretaceous) tectonic elements which include the Anambra Basin, Abakaliki uplift and the Afikpo syncline. In the east and west respectively, the Cameroon volcanic line and the Dahomey Basin mark the bounds of the Delta. The Cenozoic Niger Delta is situated at the intersection of the Benue trough and the South Atlantic Ocean where a triple junction developed during the separation of South America from Africa [3,4]. The delta is considered one of the most prolific hydrocarbon provinces in the world, and recent giant oil discoveries in the deep-water areas suggest that this region will remain a focus of exploration activities [5].

The Niger Delta is also one of the largest regressive deltas in the world [6] and considered a classical shale tectonic province. From the Eocene to the present, the delta has prograded southwestward, forming depo-belts that represent the most active portion of the delta at each stage of its development. These depo-belts has an area of about 300,000 sq km [7], a sediment volume of 500,000 cubic km [8] and sediment thickness of over 10 km in the basin depocenter [9].

2. DATA SET AND METHODOLOGY

2.1 Dataset

The dataset available for this study include:

1. Three-dimensional (3-D) seismic data
2. 5 Wells (UDI_01, UDI_02, UDI_03, UDI_04 and UDI_05) with different log data.
3. 1 check shot survey for UDI_03
4. Deviation survey for all the wells

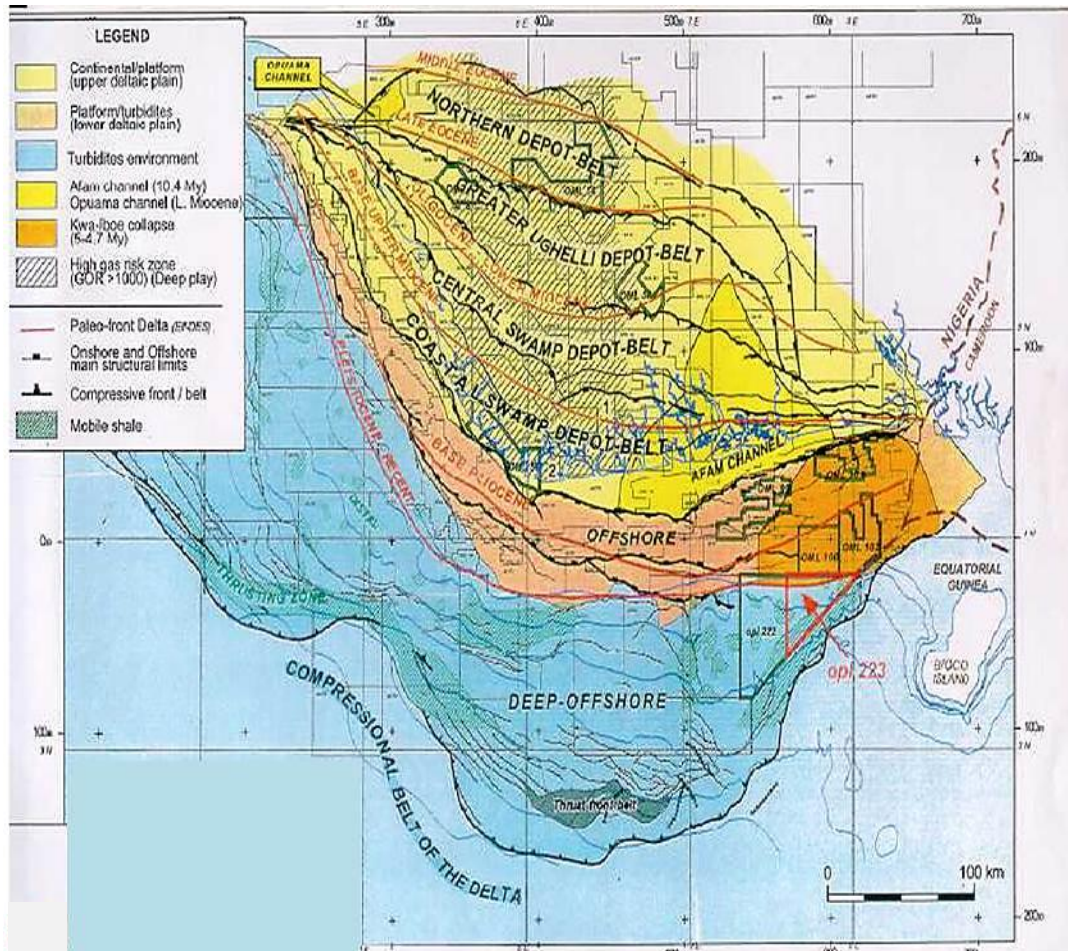


Fig. 1. Regional setting of Niger Delta depobelts [10]

The 3-D seismic data which was in SEG-Y format, consisting of 400 in-lines and 220 cross-lines, covering an aerial extent of 42.62 Km² was imported into Petrel software (Fig. 3). To cover the study area, the seismic data was interpreted at a step increment of 5 intervals on both in-lines and cross-lines.

The well log data, which was in ASCII format was also imported into the software. This consists of two different data, the well header, which carries the names and coordinates of the wells and the petrophysical data, which comprise the different log types.

Wellhead, deviation surveys and well logs were all imported in their correct formats.

2.2 Well Correlation

Four (4) reservoir sand units (Sand A100, Sand A125, Sand A150 and Sand A200) were

identified and correlated based on the backstepping (low reading) of GR log and a high deflection to the right of deep resistivity log. These reservoirs are taken to be potentially hydrocarbon-bearing. The line of correlation is chosen, such that it follows an NW-SE trend for better imaging of the subsurface structure and deposition trend (Fig. 4).

2.3 Seismic Interpretation

The potential reservoirs identified on well logs were tied to the seismic data using the available check shot data to generate a synthetic seismogram. The corresponding seismic events were then interpreted through on inlines and crosslines on an increment of 5. The resulting seismic horizons were then converted to time structure maps using a convergent Interpolation Algorithm. The surfaces were smoothed, and then depth converted to depth structure maps using the Time-Depth relationship obtained from

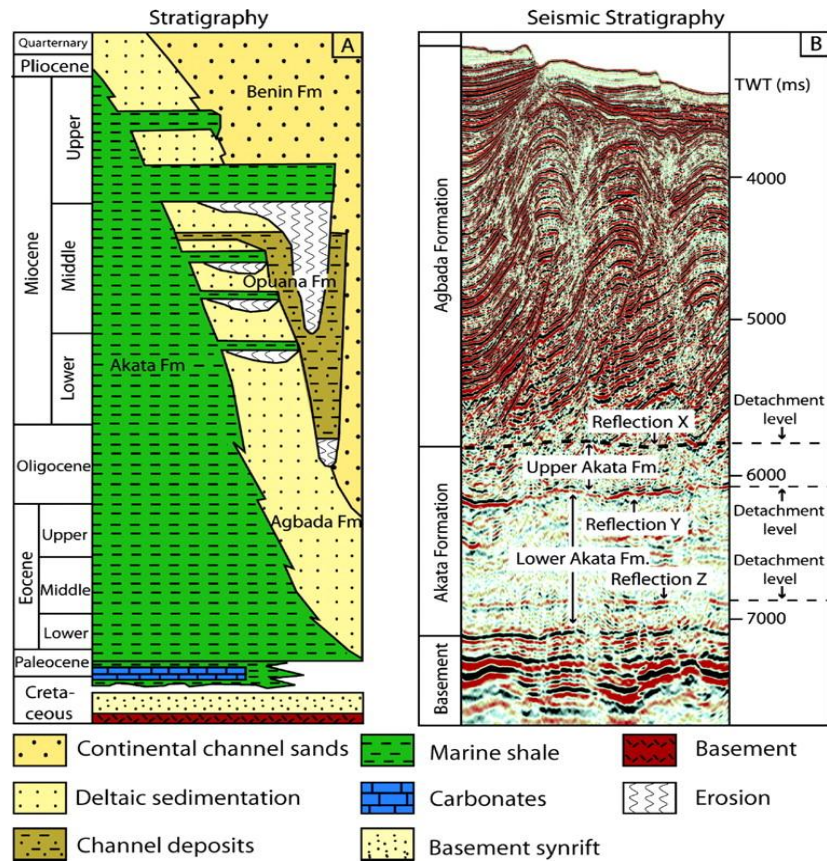


Fig. 2. Niger Delta formations and their epoch [11]

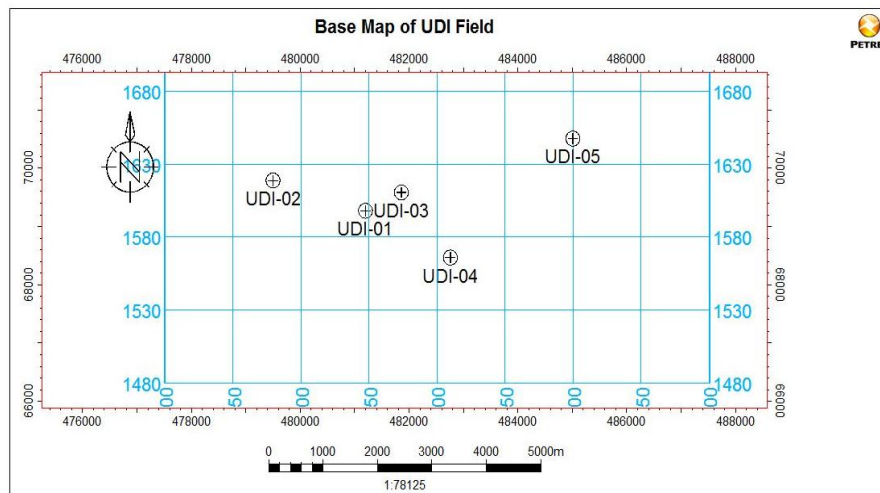


Fig. 3. Base map of UDI field showing the well locations and the survey extent

the Check shot data. Structural interpretation of the seismic data was done. Seven different faults labeled Flt 1, Flt 2, Flt 3, Flt 4, Flt 5, Flt 6, Flt 7

were interpreted through the seismic volume. Of these faults, two (Flt 1 and Flt 2) are major faults while the others are minor faults.

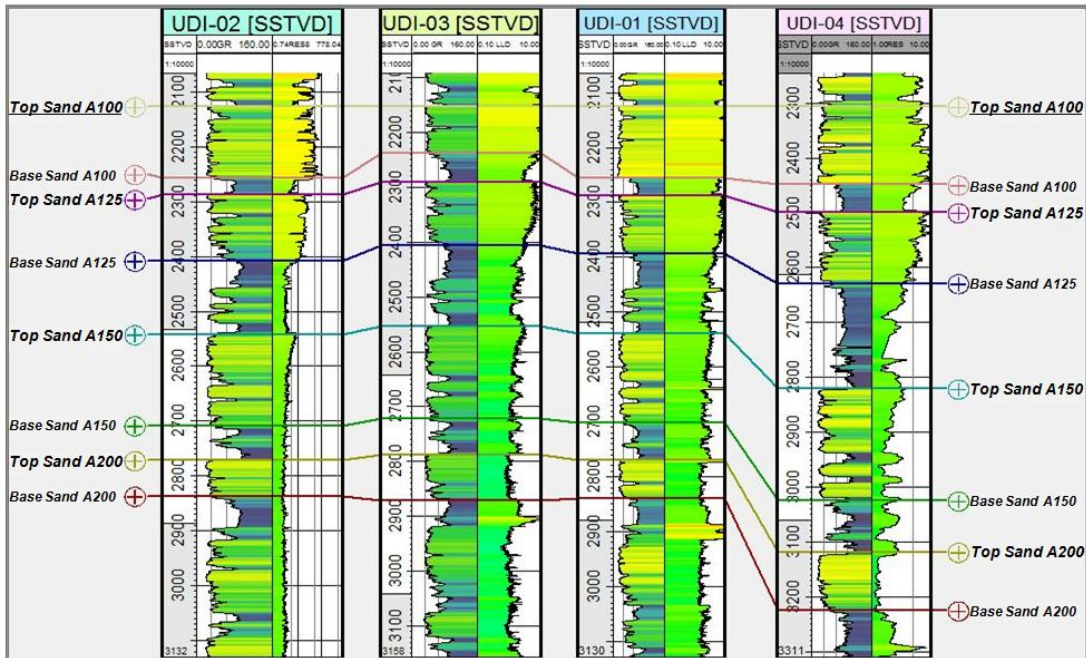


Fig. 4. Well correlation panel for wells UDI-01, UDI-02, UDI-04 and UDI-07

2.4 Lithofacies Distribution from the Digitized Well LOGS

In the course of this research, the lithofacies are identified based on the GR log. Sands commonly have relatively low GR and high effective porosity response while shales and clay-rich lithologies usually do have a relatively high GR and low effective porosity response. A discrete lithofacies log was generated by inputting a line of code in the log calculator in Petrel™. The line of code is as given below:

Lithofacies=if(GR<60,0,1): Where GR reading less than 55 is means a sandy interval (assigned a yellow color), with code '0' while GR reading greater than 55 means a shaly lithology (black color) with code '1'.

The GR baseline value of 60 was arrived at after careful study and analysis of the GR log signature across the depth and in all the four wells available for this research.

Fault modeling and Pillar gridding: Fault sticks were defined in the seismic section to indicate the dip of the faults. Fault polygons were then produced from the fault sticks and were depth converted. The depth converted fault polygons were then used to generate fault pillars. Series of key pillars were joined laterally to indicate the shape and the extent of the faults.

3. RESULTS AND DISCUSSION

To adequately characterize UDI Field as it relates to the hydrocarbon potential, detailed well log interpretation and analysis, as well as robust seismic interpretation, were integrated. The four potential reservoir intervals delineated were adequately characterized, and one of them (Sand A125) was taken as the representative interval for modeling.

3.1 Well Correlation

It is essential to establish the continuity and lateral extent of the potential sands hosting hydrocarbon within the field. To achieve this, a careful well log correlation was carried out using a combination of GR log and Resistivity log in all the four wells (Fig. 4). This is arrived at by combining areas of low GR log reading (backstepping of the GR log curve) with areas of high resistivity log reading. The GR indicates lithology i.e., it discriminates between the reservoir and non-reservoir interval.

3.2 Seismic Interpretation

Four (4) horizons were mapped, labelled Top Sand A100, Top Sand A125, Top Sand A150 and Top Sand A200, on both inlines and crosslines on an increment of 5 (Fig. 5). The resulting horizons were converted to time

structure maps (Fig. 5) using a convergent interpolation method. The time structure maps were then converted to depth structure maps using the mathematical relationship obtained by plotting the time-depth relationship gotten from the check shot data. The resulting depth structure maps are as presented in Fig. 6. The closures identified on the time structure maps were preserved on all the depth maps.

3.3 Petrophysical Interpretation of UDI Field Reservoirs

The results of the average petrophysical parameters' estimate for all the wells are as presented in Table 1. From the values given on the table, it is observed that porosity in the Field decreases with depth i.e., Sand A 100 has the average highest porosity value of 29.4(%) while Sand A200 has the lowest value of 25.3(%). Net-to-gross ratio also follows the pattern of decreasing value with depth. Sand A150 has the

highest average gross thickness value, 170.4 m, while Sand A200 has the least thickness of 80.5 m. The net-to-gross ratio preserved the pattern of gross thickness, and this resulted in Sand A150 still having the highest Net thickness and Sand A200 having the least Net sand thickness. The relatively large net sand thicknesses, high net-to-gross ratio values, and the high porosity values all support the reservoir intervals within the UDI Field to be of good quality.

Lithofacies model of sand A125: The lithofacies are distributed throughout the depth-converted grid. The lithofacies model of Sand A125 shows areas of good sand development and areas dominated by shale within the reservoir. The model revealed the reservoir to be of a high relief (Fig. 7). Different layers of the model were studied, and it was observed that there are changes in the positions of the sand and shale development, both spatially and temporally.

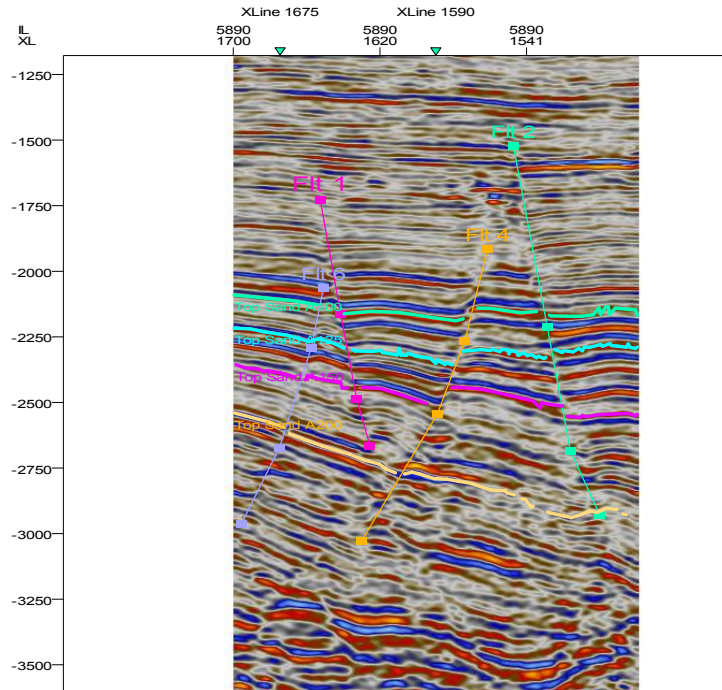


Fig. 5. Seismic section inline 5890 showing the interpreted horizons and some of the interpreted faults

Table 1. Average petrophysical estimates across the four wells

Reservoir	Gross thickness (m)	NTG (%)	Vsh(%)	Net sand (m)	Porosity (%)
Sand A100	122.5	88.1	11.9	107.9	29.4
Sand A125	117.3	84.6	15.4	99.2	28.4
Sand A150	170.4	82.4	17.6	140.4	26.9
Sand A200	80.5	76.2	23.8	61.3	25.3

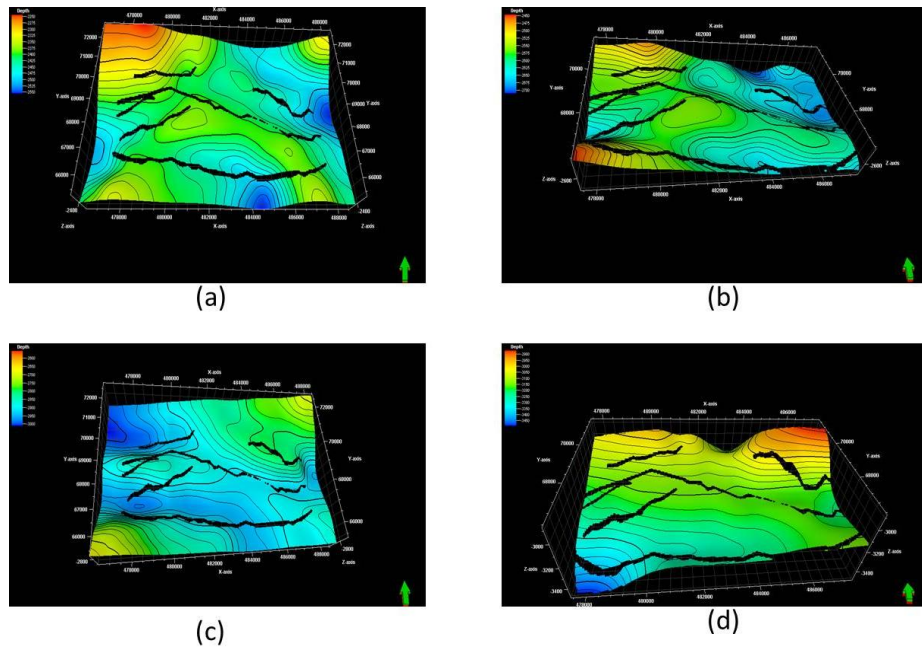


Fig. 6. Depth structure map of (a) Sand A100, (b) Sand A125, (c) Sand A150 and (d) Sand A200

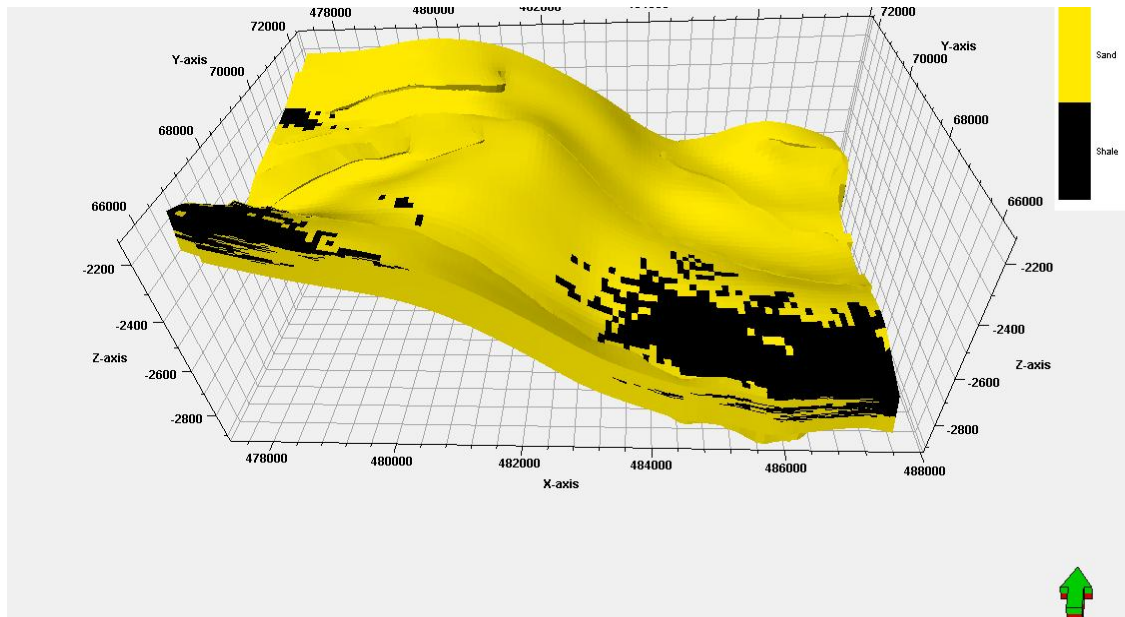


Fig. 7. 3D static lithofacies model of sand A125

Petrophysical modeling of sand A125: Three petrophysical properties, including the Volume of shale, porosity and the net-to-gross ratio was built based on the petrophysical modeling workflow adopted.

The Volume of Shale (Vsh) model: The volume of shale Model (Fig. 8) represents the distribution of the upscaled volume of shale property in the

3D grid. Each cell in the grid represents a value of the shale volume in Sand A125. Areas with purple coloration are the areas with the least volume of shale value corresponding to good reservoir facies.

Net-to-Gross ratio model: The net-to-gross ratio model (Fig. 9) represents the distribution of the upscaled net-to-gross ratio (NTG) property in

the 3D grid. Each cell in the grid represents a value of the net sand in Sand B. Studying the distribution, it is observed that areas in the northwestern-southeastern belt of the model have high net-to-gross ratio values (orange and yellow areas) and will be good targets for development consideration.

Porosity model: The porosity model (Fig. 10) represents the property distribution of the upscaled porosity log, which in turn gives a guide to the volume of the interconnected pore spaces within the reservoir. The areas with red and yellow colors are areas of high porosity. Porosity is generally high in the reservoir.

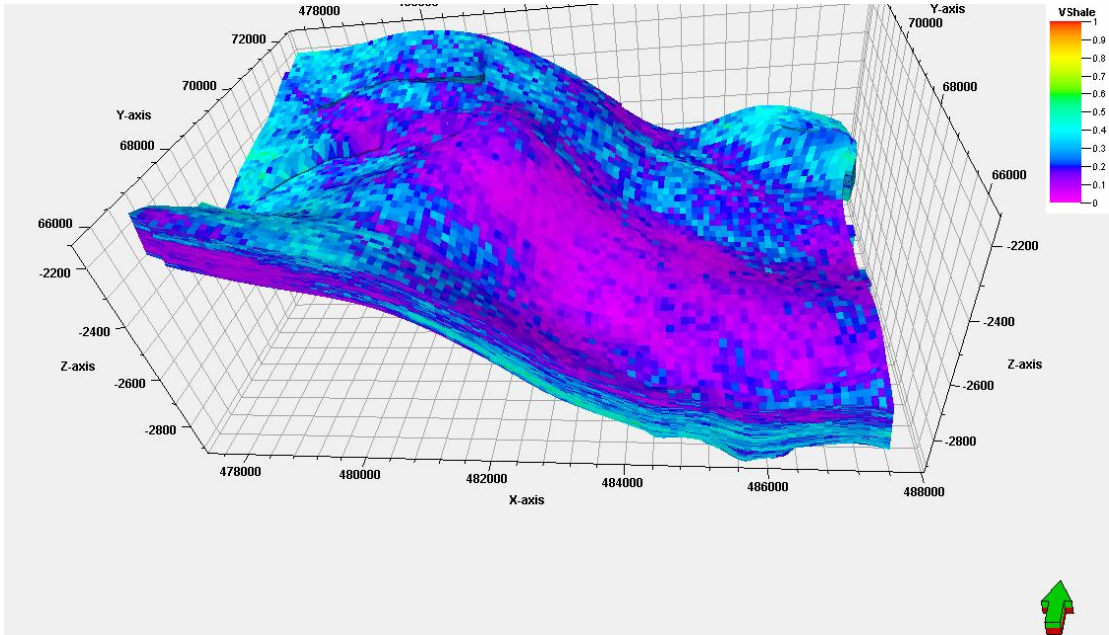


Fig. 8. Volume of shale model of sand A125

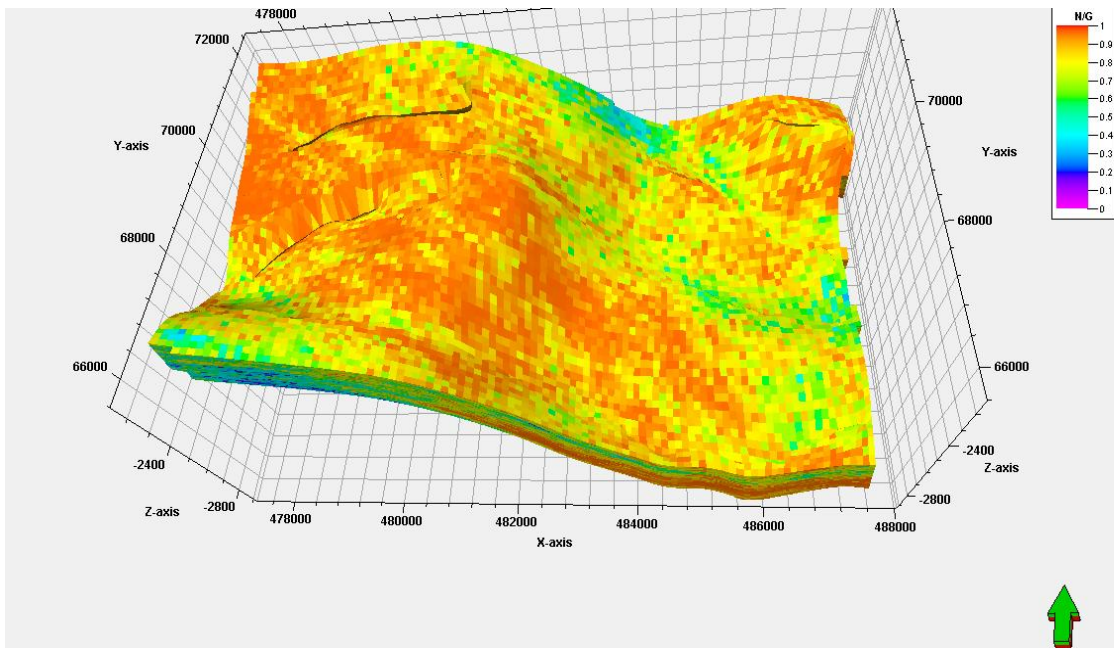


Fig. 9. Net-to-gross model of sand A125

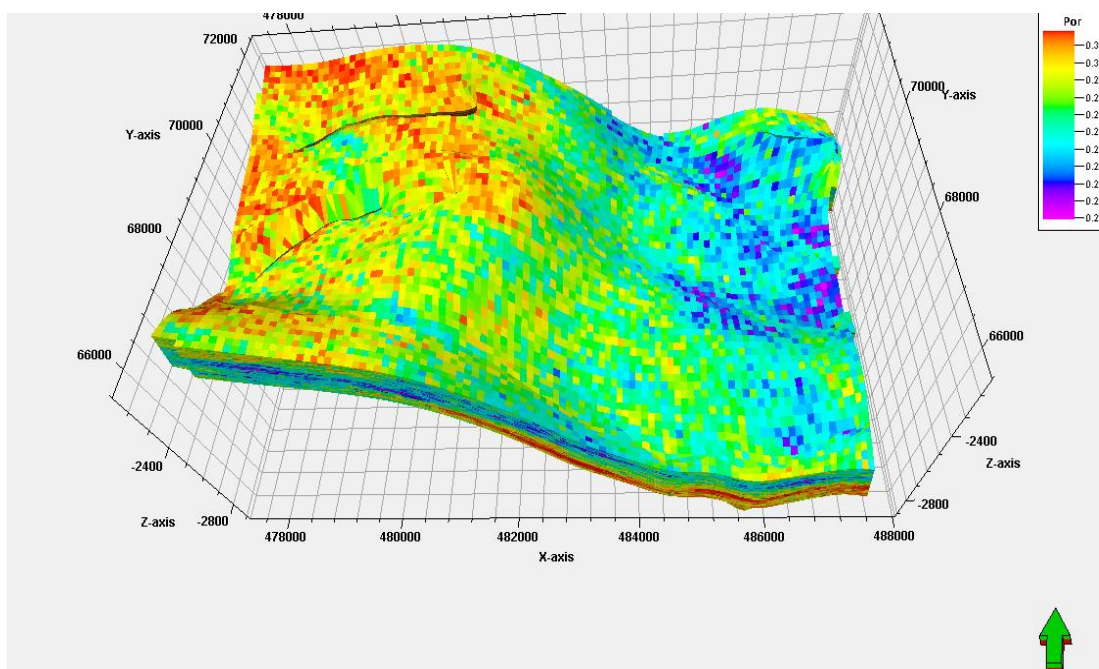


Fig. 10. Porosity model of sand A125

4. CONCLUSIONS

The four reservoir intervals identified and correlated across UDI Field have sufficient thickness, porosity and net-to-gross ratio values to qualify as a good reservoir.

The isopach maps produced show that the reservoir intervals generally thin in the northern direction, suggesting that the direction of sand development is towards the south.

The lithofacies model reveals reservoir interval Sand A125 to be of high relief. The model also shows areas of good sand distribution which corresponds to regions of favorable petrophysical properties.

The petrophysical models generated-volume of shale, porosity and net-to-gross ratio models give the petrophysical properties that are useful and required in reserve volumetrics estimation.

Quality checking of the models indicates consistency in both lithofacies and the petrophysical models in a relationship that same areas in the field with 'good' facies have high porosity, low shale volume, and high net-to-gross ratio.

Extrapolations of reservoir properties away from well control honored the geological interpretation

of reservoir Sand A125 thereby reducing the subsurface reservoir uncertainties to the minimum.

COMPETING INTERESTS

Authors have declared that no competing interests exist.

REFERENCES

1. Beka FT, Oti MN. The distal offshore Niger Delt; frontier prospects of amature-petroleum province, in Oti MN, Postma G, eds Geology of Deltas; Rotterdam AA. 1995;237-241.
2. Doust H, Omatsola E. Niger Delta: American Association of Petroleum Geologist Bulletin. 1989;48:201-238.
3. Burke K. Longshore drift, submarine canyon and submarine fans in development of Niger Delta: American Association of Petroleum Geologist Bulletin. 1972;56:1975-1983.
4. Whiteman A. Nigeria: Its Petroleum Geology, Resources and Potential: London, Gham and Trotman. 1982;394.
5. Corredor F, Shaw JH, Bilotti F. Structural styles in the deepwater fold a thrustbelts of the Niger Delta. AAPG Bulletin. 2005; 89(6):753-780.

6. Doust H, Omatsola E. Niger Delta, in Edwards JD, Santagrossi PA. eds. Divergent/Passive margin basins: American Association of Petroleum Geologist Memoir. 1990;48:239-248.
7. Kulke H. Nigeria, in Kulke H ed., Regional petroleum geology of the world, Part II: Africa, America, Australia and Antarctica: Berlin, Gebruder Bontraeger. 1995;143-172.
8. Hospers J. Gravity field and structure of the Niger Delta, Nigeria, West Africa: Geological Society of American Bulletin. 1965;76:407-422.
9. Kaplan A, Lusser CU, Norton IO. Tectonic map of the world, panel 10: Tulsa, American Association of Petroleum Geologists, scale 1:10,000,000; 1994.
10. Dessauvage TFG. Explanatory note to the geological map of Nigeria; 1975.
11. Lawrence RS, Munday S, Bray R. Regional geology and geophysics of the eastern gulf of Guinea (Niger Delta). The Leading Edge. 2002;1112-1117.

© 2020 *Osuya and Ayorinde*; This is an Open Access article distributed under the terms of the Creative Commons Attribution License (<http://creativecommons.org/licenses/by/4.0>), which permits unrestricted use, distribution, and reproduction in any medium, provided the original work is properly cited.

Peer-review history:
The peer review history for this paper can be accessed here:
<http://www.sdiarticle4.com/review-history/55238>